

## Thermodynamic Properties of $\text{Co}_3\text{O}_4$ and $\text{Sr}_6\text{Co}_5\text{O}_{15}$ from First-Principles

James E. Saal,\* Yi Wang, ShunLi Shang, and Zi-Kui Liu

Department of Materials Science and Engineering, The Pennsylvania State University, 304 Steidle, University Park, Pennsylvania 16802, United States

Received April 27, 2010

The Gibbs energy function of  $\text{Sr}_6\text{Co}_5\text{O}_{15}$  is calculated by first-principles for use in CALPHAD thermodynamic modeling. An efficient method is employed, using the Debye–Grüneisen model to predict the temperature dependence of the heat capacity and entropy. The equation of state from first-principles and the Debye temperature from harmonic phonon calculations by the supercell approach are taken as input. The effect of using the GGA+U approach on the results is also reported. The properties of  $\text{Co}_3\text{O}_4$  are predicted with this method to compare to experiments and quasi-harmonic phonon calculations and are shown to achieve the accuracy necessary for CALPHAD modeling.

### Introduction

The  $\text{La}_x\text{Sr}_{1-x}\text{CoO}_{3-\delta}$  perovskite has unique mixed-conducting properties that are appealing in a wide range of applications, such as solid oxide fuel cells, oxygen separation membranes, hydrocarbon oxidation, and gas sensors.<sup>1,2</sup> Tailoring of the perovskite's properties by altering chemistry and processing is necessary for implementation in practical applications. This can most efficiently be done with CALPHAD modeling of PHase Diagram (CALPHAD) modeling.<sup>3,4</sup> However, a common issue during the CALPHAD modeling of such complex, multicomponent systems is that thermodynamic properties of certain, perhaps obscure, phases have not been investigated or are not available in the literature.

One such compound is  $\text{Sr}_6\text{Co}_5\text{O}_{15}$ , which has complex phase relations with  $\text{La}_x\text{Sr}_{1-x}\text{CoO}_{3-\delta}$  between 1100 and 1200 K.<sup>5,6</sup>  $\text{Sr}_6\text{Co}_5\text{O}_{15}$  was first identified in 1995, when the low-temperature hexagonal form of  $\text{SrCoO}_3$  was determined to be a mixture of  $\text{Sr}_6\text{Co}_5\text{O}_{15}$  and  $\text{Co}_3\text{O}_4$ .<sup>7</sup> It is also a member of a series of

complex oxides that are being investigated for thermoelectric applications<sup>8–11</sup> and belongs to a family of strontium cobalt oxides with interesting physical properties.<sup>12</sup> A CALPHAD modeling of the perovskite and the La–Sr–Co–O system requires the Gibbs energy function for  $\text{Sr}_6\text{Co}_5\text{O}_{15}$ . However, no experimental thermodynamic data is known, but previous studies have resolved its crystallographic, magnetic, and electronic properties.<sup>7,11</sup>

First-principles calculations based on density functional theory have enabled the CALPHAD modeling of oxide systems where little experimental data are available<sup>13</sup> by predicting 0 K thermodynamic properties, such as the enthalpy of formation.<sup>4</sup> However, such data alone is insufficient to accurately determine the complete, temperature-dependent Gibbs energy function of a phase. Other experimental data, such as the melting point, must be used to evaluate the remaining model parameters. An ideal approach is to determine finite-temperature thermochemical properties from first-principles. Quasi-harmonic phonon calculations by the supercell method are often employed to do so,<sup>14–16</sup> but such calculations can be computationally expensive for the complex structures that are often found in multicomponent oxide systems, such as  $\text{Sr}_6\text{Co}_5\text{O}_{15}$ . Simpler models can be used to approximate these properties, such as the Debye–Grüneisen model,<sup>17,18</sup> but estimates for the errors in employing such

\*To whom correspondence should be addressed. E-mail: jes531@psu.edu.

- (1) Kharton, V. V.; Yaremchenko, A. A.; Naumovich, E. N. *J. Solid State Electrochem.* **1999**, *3*, 303.
- (2) Kolesnik, S.; Dabrowski, B.; Mais, J.; Majjiga, M.; Chmaissem, O.; Baszczuk, A.; Jorgensen, J. D. *Phys. Rev. B* **2006**, *73*, 214440.
- (3) Kaufman, L.; Bernstein, H. *Computer Calculation of Phase Diagrams*; Academic Press: New York, 1970.
- (4) Liu, Z. K. *J. Phase Equilib. Diffus.* **2009**, *30*, 517.
- (5) Cherepanov, V. A.; Barkhatova, L. Y.; Petrov, A. N.; Voronin, V. I. Phase Equilibria in the La–Sr–Co–O System and Thermodynamic Stability of the Single Phases. *Proceedings of the International Symposium on Solid Oxide Fuel Cells*; Electrochemical Society, Yokohama, Japan, June 18–23, 1995; p 434.
- (6) Vashook, V. V.; Zinkevich, M. V.; Zonov, Y. G. *Solid State Ionics* **1999**, *116*, 129.
- (7) Harrison, W. T. A.; Hegwood, S. L.; Jacobson, A. J. *J. Chem. Soc., Chem. Commun.* **1995**, 1953.
- (8) Iwasaki, K.; Ito, T.; Matsui, T.; Nagasaki, T.; Ohta, S.; Koumoto, K. *Mater. Res. Bull.* **2006**, *41*, 732.
- (9) Iwasaki, K.; Murase, T.; Ito, T.; Yoshino, M.; Matsui, T.; Nagasaki, T.; Arita, Y. *Jpn. J. Appl. Phys.* **2007**, *46*, 256.
- (10) Iwasaki, K.; et al. *J. Alloys Compd.* **2004**, *377*, 272.

- (11) Sun, J. L.; Li, G. B.; Li, Z. F.; You, L. P.; Lin, J. H. *Inorg. Chem.* **2006**, *45*, 8394.
- (12) Lee, K. W.; Pickett, W. E. *Phys. Rev. B* **2006**, *73*, 174428.
- (13) Saal, J. E.; Shin, D.; Stevenson, A. J.; Messing, G. L.; Liu, Z. K. *J. Am. Ceram. Soc.* **2008**, *91*, 3355.
- (14) Arroyave, R.; Shin, D.; Liu, Z. K. *Acta Mater.* **1809**, *53*, 2005.
- (15) Golunbfskie, W. J.; Arroyave, R.; Shin, D.; Liu, Z. K. *Acta Mater.* **2006**, *54*, 2291.
- (16) Wang, Y.; Liu, Z. K.; Chen, L. Q. *Acta Mater.* **2004**, *52*, 2665.
- (17) Moruzzi, V. L.; Janak, J. F.; Schwarz, K. *Phys. Rev. B* **1988**, *37*, 790.
- (18) Shang, S.-L.; Wang, Y.; Kim, D.; Liu, Z.-K. *Comput. Mater. Sci.* **2010**, *47*, 1040.

models are necessary to determine if the resulting predictions are suitably accurate for CALPHAD modeling.

In the current paper, the thermochemical properties of  $\text{Sr}_6\text{Co}_5\text{O}_{15}$  from first-principle calculations will be discussed, employing the Debye–Grüneisen model where an input parameter is derived from harmonic phonon calculations at the equilibrium volume. This approach is first used to predict the properties of  $\text{Co}_3\text{O}_4$ , where experimental data is available.<sup>19–22</sup> Quasi-harmonic phonon calculations are also performed on  $\text{Co}_3\text{O}_4$  to test the accuracy of the phonon supercell approach with  $\text{Co}_3\text{O}_4$ .  $\text{Co}_3\text{O}_4$  is an appropriate benchmark for  $\text{Sr}_6\text{Co}_5\text{O}_{15}$  as both have antiferromagnetic ordering with similar Néel transformation temperatures, and both contain Co ions with two unique charge valences.<sup>11,19</sup> It is shown that this approach for predicting the thermodynamics of transition metal, multi-component oxides is sufficiently accurate for determining their CALPHAD Gibbs energy functions. The thermochemical properties of  $\text{Sr}_6\text{Co}_5\text{O}_{15}$  are then predicted and used in a CALPHAD modeling of its Gibbs energy function.

### Methodology

The temperature- and volume-dependent free energy of a solid system,  $F(V, T)$ , can be defined by

$$F(V, T) = E_0(V) + F_{\text{vib}}(V, T) + F_{\text{el}}(V, T) + F_{\text{def}}(V, T) \quad (1)$$

Where  $E_0(V)$  is the static 0 K energy,  $F_{\text{vib}}(V, T)$  the vibrational free energy,  $F_{\text{el}}(V, T)$  the thermal electronic free energy, and  $F_{\text{def}}(V, T)$  the contribution from point defects in the structure. In the current work,  $E_0(V)$  is determined by first-principles calculations.  $F_{\text{el}}(V, T)$  is assumed to be negligible since  $\text{Co}_3\text{O}_4$  and  $\text{Sr}_6\text{Co}_5\text{O}_{15}$  are semiconductors with large resistivity at low temperatures.<sup>10,23</sup>  $F_{\text{def}}(V, T)$  is ignored in the case of  $\text{Co}_3\text{O}_4$  as no significant quantity of point defects has been reported. Oxygen vacancies have been observed for  $\text{Sr}_6\text{Co}_5\text{O}_{15}$ , on the order of 2%,<sup>9</sup> which are expected to have a small effect on the free energy.

$F_{\text{vib}}(V, T)$  is determined by the Debye–Grüneisen model.<sup>17</sup> Within this model, the vibrational contribution to the free energy is defined as

$$F_{\text{vib}}(V, T) = \frac{9}{8} k_{\text{B}} \theta_{\text{D}}(V) - k_{\text{B}} T \left[ D\left(\frac{\theta_{\text{D}}(V)}{T}\right) + 3 \ln\left(1 - e^{-\theta_{\text{D}}(V)/T}\right) \right] \quad (2)$$

where  $k_{\text{B}}$  is Boltzmann's constant and  $\theta_{\text{D}}$  the volume-dependent Debye temperature.  $D(x)$  is the Debye function, defined as

$$D(x) = \frac{3}{x^3} \int_0^x \frac{z^3 dz}{e^z - 1} \quad (3)$$

The volume-dependent Debye temperature can be approximated by

$$\theta_{\text{D}}(V) = s A V_0^{1/6} \left(\frac{B_0}{M}\right)^{1/2} \left(\frac{V_0}{V}\right)^{\gamma} \quad (4)$$

where  $V_0$  is the ground state volume,  $M$  the molecular weight,  $\gamma$  the Grüneisen parameter,  $B_0$  the bulk modulus,  $A$  a constant  $(6\pi^2)^{1/3} \hbar / k_{\text{B}}$ , and  $s$  a scaling parameter that relates the average sound velocity to the bulk modulus and effectively scales the Debye temperature. The Grüneisen parameter can be defined by

$$\gamma = \frac{1}{2} (1 + B'_0) - x \quad (5)$$

where  $B'_0$  is the derivative of the bulk modulus with pressure and  $x$  a parameter taken to be either 1 or 2/3 if below or above the Debye temperature, respectively. The high temperature value is used in this work since high temperature data have the largest effect on the Gibbs energy function in the CALPHAD modeling.  $V_0$ ,  $B_0$ , and  $B'_0$  are predicted in the current work by calculating the equation of state (EOS) from first-principles.

As the goal of this work is to determine the thermochemical properties from first-principles, free parameters such as  $s$  must also be determined from first-principles. Previous work has found that a value of 0.617 for this parameter worked best to reproduce the experimental bulk modulus for 4d cubic nonmagnetic transition metal elements.<sup>17</sup> However, this value has not been proven to be universal and may be greatly different for other classes of materials, such as transition metal oxides.<sup>24</sup> A solution we propose is to predict the Debye temperature of the material from harmonic phonon calculations at the ground state volume by

$$\theta_{\text{D}}(n) = \frac{\hbar}{k_{\text{B}}} \left[ \frac{1}{3} (n+3) \sum_j \frac{\omega_j^n}{3pN} \right]^{1/n} \quad (6)$$

where  $n$  is the Debye temperature moment,  $3pN$  the number of vibrational degrees of freedom, and  $\omega_j$  the vibrational frequency of mode  $j$ .<sup>24</sup> The Debye temperature of  $n = 2$  (discussed in more detail in the next Section) is then used to fit the scaling parameter. Phonon calculations at only the ground state volume are much less computationally expensive than quasi-harmonic phonon calculations, which are carried out at multiple volumes, and can be readily applied to complex systems, such as  $\text{Sr}_6\text{Co}_5\text{O}_{15}$ . The effect of  $s$  on the thermochemical properties will be examined.

The spinel  $\text{Co}_3\text{O}_4$  is used to test this method for predicting the thermochemical properties of a transition metal oxide since experimental data is available for comparison. Several cases are tested using this approach to estimate potential sources of error. The influence of the magnetic state on the thermochemical properties are investigated by calculating the properties of both the antiferromagnetic (AFM) 0 K ground state<sup>25</sup> and the metastable nonmagnetic (NM) state of  $\text{Co}_3\text{O}_4$ . The effect of charge localization is often cited as an

(19) Ikedo, Y.; Sugiyama, J.; Nozaki, H.; Itahara, H.; Brewer, J. H.; Ansaldo, E. J.; Morris, G. D.; Andreica, D.; Amato, A. *Phys. Rev. B* **2007**, *75*, 054424.

(20) Khriplovich, L. M.; Kholopov, E. V.; Paukov, I. E. *J. Chem. Thermodyn.* **1982**, *14*, 207.

(21) King, E. G. *J. Am. Chem. Soc.* **1957**, *79*, 2399.

(22) Mocala, K.; Navrotsky, A.; Sherman, D. M. *Phys. Chem. Miner.* **1992**, *19*, 88.

(23) Koumoto, K.; Yanagida, H. *J. Am. Ceram. Soc.* **1981**, *64*, C156.

(24) Anderson, O. *Equations of state of solids for geophysics and ceramic science*; Oxford University Press: New York, 1995.

(25) Roth, W. L. *J. Phys. Chem. Solids* **1964**, *25*, 1.

important consideration when investigating the properties of transition metal oxides with density functional theory.<sup>26</sup> Such effects are typically taken into consideration by incorporating the so-called GGA+U approach,<sup>27</sup> where an intra-atomic interaction energy,  $U$ , is added on site of the given ion. However, this approach adds the free parameter  $U$  to the calculation. The GGA+U approach was shown to be necessary in reproducing the experimental oxidation energies of transition metal unary oxides, such as  $\text{Co}_3\text{O}_4$ .<sup>26</sup> In that study, the values of the parameter  $U$  were determined by fitting to the experimental oxidation energies. These values were later applied to several transition metal lanthanide perovskites, where the use of the GGA+U approach brought the calculated enthalpies of formation of the perovskites, including  $\text{LaCoO}_3$ , closer to experiments.<sup>28</sup> The effect of using the GGA+U approach on predicting the finite-temperature thermochemical properties with the Debye–Grüneisen model is determined in this work by comparing results with and without GGA+U, using the fitted  $U$  value for Co.<sup>26</sup> Lastly, the importance of using harmonic phonon calculations to determine the scaling parameter in the Debye–Grüneisen model is examined by comparing the results from the parameter 0.617 with those from the phonon-predicted parameter and from scaling parameters fitted to the experimental Debye temperature of  $\text{Co}_3\text{O}_4$ .

Spin-polarized density functional theory calculations are performed with the Vienna Ab Initio Simulation Package (VASP).<sup>29</sup> The pseudopotentials supplied with VASP are used with the projected augmented wave method<sup>30</sup> and the generalized gradient approximation<sup>31</sup> of Perdew, Burke, and Ernzerhof.<sup>32</sup> GGA+U calculations employ Dudarev's approach,<sup>27</sup> which requires as input the difference of the on site Coulomb interaction energy,  $U$ , and a separate exchange interaction energy,  $J$ . The previously determined  $U-J$  value of 3.3<sup>26</sup> is used for Co. Calculations for the 0 K ground states of  $\text{Co}_3\text{O}_4$  and  $\text{Sr}_6\text{Co}_5\text{O}_{15}$  are carried out by relaxing all degrees of freedom, with the total energies and volumes converged to within less than 1 meV and 0.1 Å<sup>3</sup> per atom, respectively. An  $8 \times 8 \times 8$  k-point matrix with a Monkhorst–Pack scheme is used for calculations of the ground state and EOS for the 14 atom primitive cell of  $\text{Co}_3\text{O}_4$ , and a  $6 \times 6 \times 6$  Monkhorst–Pack scheme for the 26 atom primitive cell of  $\text{Sr}_6\text{Co}_5\text{O}_{15}$ . The energy versus volume curve is determined by fixed volume calculations, upon which the four parameter Birch–Murnaghan EOS<sup>33</sup> in its linear form<sup>18</sup> was fit, given below:

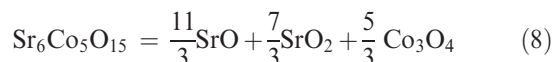
$$E(V) = a + bV^{-2/3} + cV^{-4/3} + dV^{-2} \quad (7)$$

For cases where the magnetic moments of the system go to zero with decreasing volume, only those volumes that retain

the magnetic moment are included in the EOS fit.<sup>34</sup> The ranges of volumes used in the fittings are shown in Table 1 and Table 2.

Phonon calculations by the supercell approach are performed with VASP and ATAT code<sup>35,36</sup> on the ground state volumes of  $\text{Co}_3\text{O}_4$  and  $\text{Sr}_6\text{Co}_5\text{O}_{15}$ . A supercell of 56 atoms is used for the phonon calculations of  $\text{Co}_3\text{O}_4$  with a  $4 \times 4 \times 4$  Monkhorst–Pack k-point matrix. Similarly, the 26 atom primitive cell is used for phonon calculations of  $\text{Sr}_6\text{Co}_5\text{O}_{15}$  with a  $6 \times 6 \times 6$  Monkhorst–Pack k-point matrix. The phonon-derived Debye temperature is then used to fit the scaling parameter  $s$  of the Debye–Grüneisen model, from which the heat capacity and the entropy as functions of temperature are predicted. To further probe the accuracy of the harmonic phonon calculation, a quasi-harmonic phonon calculation of  $\text{Co}_3\text{O}_4$  is performed with three additional volumes, one below and two above the ground state volume. The AFM state without GGA+U is used to ensure the mechanical stability of the structure, an issue discussed in detail in a later section.

The enthalpy of formation of  $\text{Sr}_6\text{Co}_5\text{O}_{15}$  is calculated to provide the proper reference states for the Gibbs energy function and make it consistent with established databases. The reference states are taken to be the component oxides SrO,  $\text{SrO}_2$ , and  $\text{Co}_3\text{O}_4$  by the following reaction:



The enthalpy of formation of  $\text{Sr}_6\text{Co}_5\text{O}_{15}$  is given by:

$$\Delta_f H_{\text{Sr}_6\text{Co}_5\text{O}_{15}} = E_{\text{Sr}_6\text{Co}_5\text{O}_{15}} - \frac{11}{3}E_{\text{SrO}} - \frac{7}{3}E_{\text{SrO}_2} - \frac{5}{3}E_{\text{Co}_3\text{O}_4} \quad (9)$$

where the  $E$  terms are the total energies of the structures, determined from first-principles, per mole of formula unit. The energy of the AFM state of  $\text{Co}_3\text{O}_4$  is used.

For use in CALPHAD thermodynamic modeling, the following function is used to describe the Gibbs energy of  $\text{Sr}_6\text{Co}_5\text{O}_{15}$ , in per mole of formula unit:<sup>4</sup>

$$G_{\text{Sr}_6\text{Co}_5\text{O}_{15}} = A + BT + CT \ln T + DT^2 + ET^{-1} \quad (10)$$

where  $A$ ,  $B$ ,  $C$ ,  $D$ , and  $E$  are fitting parameters. The thermochemical properties derived from the Debye–Grüneisen model are used to determine these parameters for  $\text{Sr}_6\text{Co}_5\text{O}_{15}$ . The heat capacity derived from the Debye–Grüneisen model is used to fit  $C$ ,  $D$ , and  $E$ , and the entropy is used to fit  $B$ . Lastly, the enthalpy of formation is used to fit  $A$ . The Gibbs energy functions for the reference states are taken from the CALPHAD modeling of the Sr–O<sup>37</sup> and Co–O<sup>38</sup> systems. The parameter fitting is performed with the Parrot module of ThermoCalc.<sup>39</sup>

(26) Wang, L.; Maxisch, T.; Ceder, G. *Phys. Rev. B* **2006**, *73*, 195107.  
 (27) Dudarev, S. L.; Botton, G. A.; Savrasov, S. Y.; Humphreys, C. J.; Sutton, A. P. *Phys. Rev. B* **1998**, *57*, 1505.  
 (28) Lee, Y. L.; Kleis, J.; Rossmel, J.; Morgan, D. *Phys. Rev. B* **2009**, *80*, 224101.  
 (29) Kresse, G.; Furthmüller, J. *Comput. Mater. Sci.* **1996**, *6*, 15.  
 (30) Kresse, G.; Joubert, D. *Phys. Rev. B* **1999**, *59*, 1758.  
 (31) Perdew, J. P.; Chevary, J. A.; Vosko, S. H.; Jackson, K. A.; Pederson, M. R.; Singh, D. J.; Fiolhais, C. *Phys. Rev. B* **1992**, *46*, 6671.  
 (32) Perdew, J. P.; Burke, K.; Ernzerhof, M. *Phys. Rev. Lett.* **1996**, *77*, 3865.  
 (33) Birch, F. *Phys. Rev.* **1947**, *71*, 809.  
 (34) Saal, J. E.; Shang, S.; Wang, Y.; Liu, Z. K. *J. Phys.: Condens. Matter* **2010**, *22*, 096006.

(35) van de Walle, A.; Asta, M.; Ceder, G. *CALPHAD: Comput. Coupling Phase Diagrams Thermochem.* **2002**, *26*, 539.  
 (36) van de Walle, A.; Ceder, G. *J. Phase Equilib.* **2002**, *23*, 348.  
 (37) Risold, D.; Hallstedt, B.; Gauckler, L. J. *Calphad-Comput. Coupling Ph. Diagrams Thermochem.* **1996**, *20*, 353.  
 (38) Chen, M.; Hallstedt, B.; Gauckler, L. J. *J. Phase Equilib.* **2003**, *24*, 212.  
 (39) Andersson, J. O.; Helander, T.; Hoglund, L. H.; Shi, P. F.; Sundman, B. *CALPHAD: Comput. Coupling Phase Diagrams Thermochem.* **2002**, *26*, 273.

**Table 1.** Predicted Properties of AFM and NM  $\text{Co}_3\text{O}_4$  with and without the GGA+U Correction<sup>a</sup>

	AFM	AFM+U	NM	NM+U	Exp.
$E - E^{\text{AFM(+U)}}$ [meV/atom]	0	0	96	380	
8a magnetic moment	2.31	2.66	0	0	3.26 <sup>25</sup>
$a$ [Å] (% error)	8.106 (0.27)	8.152 (0.84)	8.048 (-0.45)	8.041 (-0.53)	8.084 <sup>19</sup>
EOS V range [fraction of $V_0$ ]	0.68–1.72	0.51–1.33	0.34–1.33	0.51–1.33	
$B_0$ [GPa]	204.5	198.5	241.0	213.2	
$B_0'$	4.692	4.196	4.242	4.358	
$\theta_D$ [K]	784	759	719	unstable	525 <sup>25</sup>
scaling parameter $s$	0.956	0.936	0.811	unstable	0.640

<sup>a</sup> The 8a Co magnetic moment corresponds to the magnitude of the moment found on the AFM ordered sites at the ground state volume. The 16a Co sites have no magnetic moment. The listed energy differences are between AFM and NM with the same U value.

**Table 2.** Predicted Properties by First-Principles Calculations for the Four Converged States of  $\text{Sr}_6\text{Co}_5\text{O}_{15}$ : FM with and without GGA+U, Two AFM States, and NM with and without GGA+U<sup>a</sup>

	FM	FM+U	NM	NM+U	AFM1+U	AFM2+U	Exp.
3b	0.835	1.531	0	0	0.002	1.588	
6c1 1	0.451	0.528	0	0	0.876	-0.526	
6c1 2	0.451	0.528	0	0	-0.876	-0.526	
6c2 1	0.417	0.032	0	0	0.197	-0.014	
6c2 2	0.417	0.032	0	0	-0.196	-0.014	
net moment	3	3	0	0	0	1	
$a$ [Å] (% error)	9.6096 (1.12)	9.5956 (0.96)	9.5938 (0.95)	9.5782 (0.79)	9.6265 (1.29)	9.5982 (1.00)	9.5035 <sup>7</sup>
$c$ [Å] (% error)	12.4579 (0.49)	12.4164 (0.16)	12.5270 (1.05)	12.5382 (1.14)	12.3850 (-0.09)	12.4189 (0.18)	12.3966 <sup>7</sup>
$E - E^{\text{FM(+U)}}$ [meV/atom]	0	0	13	24	19	0.05	
EOS V range [fraction of $V_0$ ]	0.84–1.34	0.78–1.26	0.73–1.33	0.73–1.26			
$B_0$ [GPa]	112.7	103.0	98.9	102.8			
$B_0'$	5.050	4.901	4.701	4.231			
$\theta_D$ [K]	669	unstable	672	662			
scaling parameter $s$	1.142	1.191	1.219	1.178			
$\Delta H_f$ (oxides) [meV/atom]	-194.09	-79.257	-181.58	-55.487			
([kJ/mol-form])	(-486.88)	(-198.82)	(-455.50)	(-139.193)			

<sup>a</sup> The scaling parameter for FM with the GGA+U correction was fitted to the Debye temperature of the FM calculation.

## Results and Discussion - $\text{Co}_3\text{O}_4$

$\text{Co}_3\text{O}_4$  has the spinel structure ( $Fd\bar{3}m$ ) in which Co resides on two distinct Wyckoff sites: diamagnetic  $\text{Co}^{3+}$  ions on octahedral 16d sites and  $\text{Co}^{2+}$  ions on tetrahedral 8a sites with AFM ordering of the spin moments.<sup>19,25</sup> The  $\text{Co}^{2+}$  ions exhibit a Néel transformation from AFM ordering to paramagnetic disorder at 30 K. The  $\text{Co}^{3+}$  ions exhibit a broad low-spin to high-spin transition beginning at around 1000 K which is attributed to a spinel-type disordering of the Co ions.<sup>22</sup>

**Zero-Kelvin Properties.** Four cases of  $\text{Co}_3\text{O}_4$  are examined with first-principles: AFM and NM with and without the use of the GGA+U correction. Results of the calculations are summarized in Table 1. The AFM 0 K magnetic ground state for  $\text{Co}_3\text{O}_4$  is correctly predicted by the first-principles calculations after relaxing the structure with and without GGA+U, where the 16d sites contain no magnetic moment and the 8a sites are AFM ordered. The stability of AFM over the NM state increases by nearly a factor of 4 with the use of GGA+U, consistent with previous work where the oxidation energy of CoO to  $\text{Co}_3\text{O}_4$  was found to be strongly dependent on the value of U.<sup>26</sup> The magnitude of the AFM moments on the 8a sites are underestimated with respect to experiment<sup>25</sup> but made only slightly closer with GGA+U. Table 1 also summarizes the predicted lattice parameters, where both AFM calculations overestimate the 300 K experimental lattice parameter<sup>19</sup> and both NM cases underestimate it.

Energy versus volume curves were calculated for all four  $\text{Co}_3\text{O}_4$  test cases, shown in Figure 1. The  $\text{Co}_3\text{O}_4$  AFM

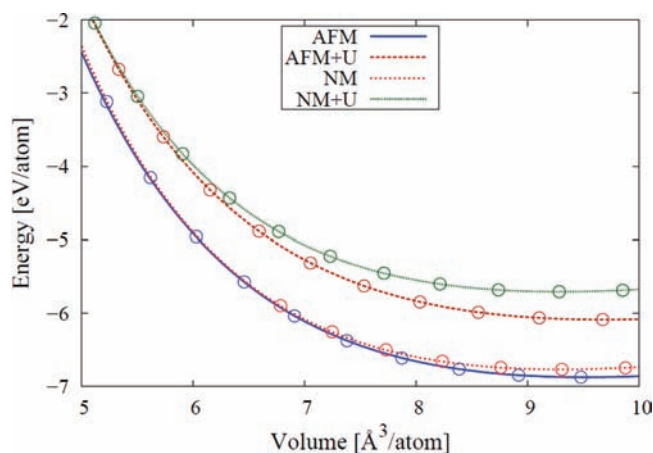


**Figure 1.** Energy versus volume for AFM and NM  $\text{Co}_3\text{O}_4$  with and without U, where points are first-principles calculations and lines are the fitted equations of state.

magnetic moments disappeared with decreasing volume. The use of GGA+U stabilized the magnetic moment to lower volumes, 4.59  $\text{Å}^3/\text{atom}$  compared to 6.03  $\text{Å}^3/\text{atom}$  without GGA+U. The parameters of the fitted equations of state are summarized in Table 1. The use of GGA+U results in predictions of a lower bulk modulus, and the NM state is predicted to have higher values than the AFM state.

**Finite-Temperature Properties.** Harmonic phonon calculations were performed on supercells of  $\text{Co}_3\text{O}_4$  to predict the Debye temperature, shown in Table 1. Differences in the

Debye temperature between the four test cases range across 60 K, with the NM case without U being the lowest at 719 K. The NM case with the GGA+U correction resulted in imaginary phonon modes, so no prediction of the Debye temperature is possible. The Debye temperature from quasi-harmonic phonon calculation varies with temperature, between 725 and 750 K above room temperature. The temperature dependence of the Debye temperature has been predicted to be strong for other spinels.<sup>40</sup> Indeed, from the current quasi-harmonic phonon calculation, the Debye temperature reaches as low as 575 K at 40 K. All the predicted values are larger than the experimental Debye temperature of 525 K,<sup>25</sup> derived from neutron scattering measurements of the temperature factor at room temperature.

The above results suggest that the difference between the calculated and measured Debye temperature is that  $\text{Co}_3\text{O}_4$  does not behave as an ideal Debye solid. The experimental value is derived from the temperature factor, whereas a Debye temperature from fitting the Debye function to calorimetric data will be different if the material is not a proper Debye solid. A test for whether this is the case is to compare the Debye temperatures derived with the  $-2$  and  $+2$  moments from the harmonic phonon calculation in eq 6. A moment of  $-2$  is related to measurement of the low frequency acoustic vibrational modes whereas  $+2$  is related to the Debye temperature derived from the heat capacity and the high temperature limit from the high frequency modes.<sup>24</sup> For an ideal Debye solid, these two temperatures would be the same. From the harmonic phonon calculation of  $\text{Co}_3\text{O}_4$  AFM without GGA+U, the  $-2$  and  $+2$  moments result in Debye temperatures of 540 K and 784 K, respectively. Therefore, the difference between the experiment and calculation is most probably due to  $\text{Co}_3\text{O}_4$  not behaving as an ideal Debye solid. Since the thermochemical properties of  $\text{Co}_3\text{O}_4$  are the focus of the current work, the Debye temperature from the  $+2$  moment, 784 K, is preferred and, when employed in the Debye–Grüneisen model, produces the best agreement with experimental heat capacity data, as shown later.

The Debye temperatures from phonon calculations and the EOS parameters from the energy versus volume curves are used in the Debye–Grüneisen model. The scaling parameters are fitted to the Debye temperatures, given in Table 1. The scaling parameters for the AFM cases with and without GGA+U are similar to one another, differing by only 0.02 (2%). The calculation of NM without GGA+U resulted in a scaling parameter of 0.811, showing that the magnetic state of the system can have a large effect on the prediction of the Debye–Grüneisen scaling parameter. These parameters are used to predict the heat capacity for  $\text{Co}_3\text{O}_4$ , shown in Figure 2. The low-temperature Néel transition and the high-temperature spin transition cannot be predicted by the Debye–Grüneisen model. However, the error in ignoring such transitions can be estimated from the excess entropy of the transition and has been found to be about 1 J/K/mol-atom for the Néel transformation at 30 K.<sup>20</sup> The peak in the heat capacity due to the high-temperature spin transition is broader and higher, so the associated excess

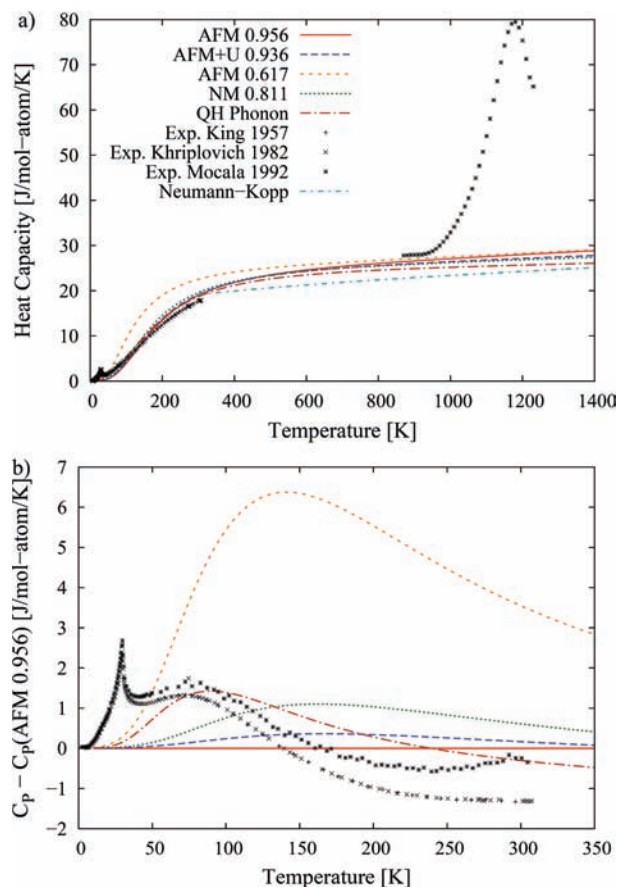


**Figure 2.** (a) Heat capacity for  $\text{Co}_3\text{O}_4$  as predicted by the Debye–Grüneisen model and quasi-harmonic (QH) phonon calculations with available experimental data<sup>19–22</sup> and (b) closeup at low temperatures, plotted with the heat capacity of the AFM state predicted with the Debye–Grüneisen model using the Debye temperature from harmonic phonon calculations taken as the reference. Numbers in the legend refer to the employed scaling parameter. The scaling parameter for AFM 0.617 is fitted for pure transition metals<sup>17</sup> and is similar to that fitted to the experimental Debye temperature.<sup>25</sup> The heat capacity predicted by the Neumann–Kopp rule is shown for comparison.

entropy is larger, about 6 J/K/mol-atom.<sup>22</sup> However, the error in ignoring this transition would only impact the thermodynamic modeling above the transition temperature, at 1000 K for  $\text{Co}_3\text{O}_4$ .<sup>22</sup>

Another commonly used approximation for the heat capacity of compounds, the Neumann–Kopp rule, assumes that the heat capacity of a compound is the weighted sum of the heat capacity of the constituent elements. The heat capacity for this approximation is calculated using heat capacity functions from the SGTE PURE database<sup>41</sup> and is shown in Figure 2. The Neumann–Kopp rule underestimates the experimental data since the heat capacity of oxygen, a gas, is much lower than that for cobalt, a solid. Another approximation would be to use the 0.617 scaling parameter,<sup>17</sup> also shown in Figure 2. This value of the scaling parameter is similar to the value obtained from the experimental Debye temperature at 525 K,<sup>25</sup> which results in 0.640. At low temperatures, the use of a scaling parameter of 0.617 greatly overestimates the heat capacity. The predictions

(40) Fang, C. M.; Loong, C. K.; de Wijs, G. A.; de With, G. *Phys. Rev. B* **2002**, *66*, 144301.

(41) Dinsdale, A. T. *CALPHAD: Comput. Coupling Phase Diagrams Thermochem.* **1991**, *15*, 317.

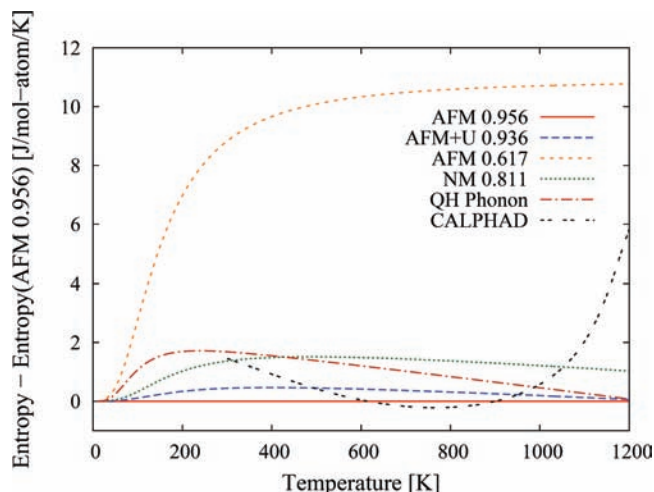


**Figure 3.** Entropies of  $\text{Co}_3\text{O}_4$  predicted using the Debye–Grüneisen model and quasi-harmonic (QH) phonon calculations with the CALPHAD modeled entropy<sup>38</sup> included for comparison, plotted with the entropy of the AFM state predicted with the Debye–Grüneisen model using the Debye temperature from harmonic phonon calculations taken as the reference. Numbers in the legend refer to the employed scaling parameter. The scaling parameter for AFM 0.617 is fitted for pure transition metals<sup>17</sup> and is similar to that fitted to the experimental Debye temperature.<sup>25</sup>

using the scaling parameters from first-principles vary slightly whether or not GGA+U is used and the magnetic state considered, as all show reasonable agreement with experiments. Closest agreement is found for the calculations from the AFM state with and without GGA+U. At high temperatures, all the Debye–Grüneisen predictions converge to similar values regardless of magnetic state, GGA+U, and scaling parameter. The quasi-harmonic phonon calculation also shows good agreement to the prediction from the Debye–Grüneisen model for AFM with and without GGA+U, suggesting that the Debye–Grüneisen model, coupled with the calculated Debye temperature, is capturing the necessary information of the oxide’s phonon spectrum to reproduce the phase’s thermochemical behavior.

Figure 3 shows the predicted entropy for  $\text{Co}_3\text{O}_4$  with the CALPHAD data,<sup>38</sup> which is derived from experimental measurements of the heat capacity. Good agreement is observed with the quasi-harmonic phonon calculation and all of the Debye–Grüneisen predictions except with the scaling parameter of 0.617 and the NM data without GGA+U. The change in the CALPHAD data at 1000 K is due to the spin transition, which, again, cannot be reproduced by the Debye–Grüneisen model. The errors for the rest of the data in the entropy appear to be on the order of 1–2 J for the predictions from the first-principles derived scaling parameters.

The use of harmonic phonon calculations to predict the Debye temperature is a necessary step for predicting the heat capacity in the Debye–Grüneisen model. Using 0.617 for the scaling parameter corresponds to a Debye temperature of 512 K, close to the experimental value of 525 K, but results in a heat capacity with large disagreement with experiment. Although the harmonic phonon predicted Debye temperature with the +2 moment does not agree with experiment, its use in the Debye–Grüneisen model gives the best agreement with experimental heat capacity measurements. In

comparison to the experimental heat capacity and entropy, the AFM case (the 0 K ground state of the compound) appears to show the best overall agreement. The influence on the predicted temperature-dependent thermochemical properties with GGA+U appears to be small, suggesting that the use of GGA+U is not necessary with the Debye–Grüneisen model and the optimum magnetic structure to employ is the 0 K magnetic ground state.

From the entropy predictions in Figure 3, the error in the entropy associated with using the Debye–Grüneisen model and the Debye temperature from harmonic phonon calculations is estimated to be on the order of 1 J/mol-atom/K, which translates to 1 kJ/mol-atom in the vibrational contribution to the Gibbs energy at 1000 K, primarily because of neglecting the Néel transformation. Such errors are the same order of magnitude typical for uncertainty in experimental thermochemical data, demonstrating that this approach is capable of predicting the properties of transition metal oxides with accuracy sufficient for CALPHAD thermodynamic modeling. The error in the entropy for  $\text{Co}_3\text{O}_4$  becomes higher at higher temperatures, on the order of 10 J/mol-atom/K, because of the spinel disordering spin transition, which is not typically found in transition metal oxides. Typically, the largest source of error in the calculation of a phase’s Gibbs energy function is from error in the enthalpy of formation. However, this error is assumed to be negligible for  $\text{Co}_3\text{O}_4$  since the U–J value employed in the current work was fitted to the experimental oxidation energy of CoO to  $\text{Co}_3\text{O}_4$  and was shown to provide an accurate prediction of the enthalpy of formation of  $\text{Co}_3\text{O}_4$ .<sup>26</sup> Another consideration is the use of eq 5 to approximate  $\gamma$ . For the AFM state without GGA+U,  $B_0'$  in Table 1 is 4.692, which results in  $\gamma = 2.2$  from eq 5 for  $x = 2/3$ . The quasi-harmonic calculation employs the thermodynamic  $\gamma$ , defined by

$$\gamma(V, T) = \frac{V(T) B(V, T) \beta(V, T)}{C_V(V, T)} \quad (11)$$

where  $\beta$  is the thermal expansion coefficient and  $C_V$  the constant volume heat capacity.<sup>42</sup> With this formulation,  $\gamma$  is about 1.3. When these two values of  $\gamma$  are used as input in the Debye–Grüneisen model, the quasi-harmonic phonon value results in a room temperature entropy about 0.5 J/mol-atom/K lower than the approximation from eq 5.

## Results and Discussion - $\text{Sr}_6\text{Co}_5\text{O}_{15}$

$\text{Sr}_6\text{Co}_5\text{O}_{15}$  has a trigonal structure ( $R\bar{3}2$ ) with three distinct Wyckoff sites for Co: 3b, 6c, and 6c.<sup>7</sup> Experimental observations of the magnetization suggest AFM ordering of the Co ions, with a Néel transformation of 25 K.<sup>11</sup> There has been no report of a high temperature spin transition such as that found in  $\text{Co}_3\text{O}_4$ .

**Zero-Kelvin Properties.** Similar to the calculations for  $\text{Co}_3\text{O}_4$ , the GGA+U correction is employed in the calculations for  $\text{Sr}_6\text{Co}_5\text{O}_{15}$  to ensure that the enthalpy of formation is accurately predicted. Calculations without the GGA+U correction are performed as well to avoid issues with mechanical instability as found in the NM case of  $\text{Co}_3\text{O}_4$ , to be discussed in more detail in the next section.

The specific local ordering of the moments for  $\text{Sr}_6\text{Co}_5\text{O}_{15}$  has not been measured experimentally. Therefore, several

(42) Wang, Y.; Li, L. *Phys. Rev. B* **2000**, *62*, 196.

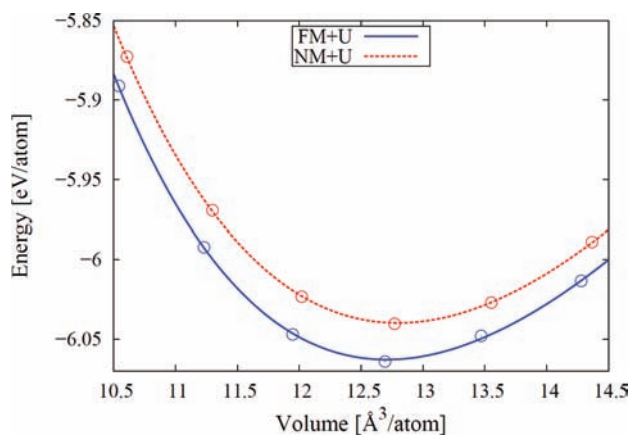


**Figure 4.** Energy versus volume for the FM+U and NM+U states of  $\text{Sr}_6\text{Co}_5\text{O}_{15}$  with points from first-principles calculations and lines from the fitted equations of state.

initial spin configurations were tested to determine the possible 0 K magnetic ground state. A ferromagnetic (FM) state, two AFM states, and the NM state converged successfully. Their magnetic configurations and energy differences with respect to FM are shown in Table 2. The predicted lattice parameters are also given in Table 2, with all four converged states overestimating the room temperature experimental parameters<sup>7</sup> by about 1%. The predicted ground state is the FM state in which the 3b site has a moment that is approximately twice that on the 6c sites, growing to a 3:1 ratio with GGA+U. Although an FM ground state is predicted, an AFM state is observed experimentally at low temperatures, based on magnetic susceptibility measurements.<sup>11</sup> This discrepancy may be attributed to an AFM state that is more energetically stable but was not found in the current work, potentially exhibiting ordering on a scale larger than the primitive cell. Furthermore, when GGA+U is employed, the AFM2 state (identical to the FM state except that 6c and 3b spin moments are in opposite directions) becomes indistinguishable in energy with FM, suggesting that the spin orientation between the two Wyckoff sites can readily change. This may be responsible for the observed 25 K Néel transformation.<sup>11</sup> Another possible contribution to the differences in the crystallographic and magnetic properties between the first-principles and experimental results is potential oxygen nonstoichiometry in the experimental studies.<sup>9</sup> The FM state is used in the next steps as it is the most stable magnetic structure. To investigate the largest possible error in using an incorrect magnetic ground state, the finite-temperature properties of NM  $\text{Sr}_6\text{Co}_5\text{O}_{15}$  are also calculated.

EOSs were fit to the calculated energy versus volume for FM and NM  $\text{Sr}_6\text{Co}_5\text{O}_{15}$ , shown in Figure 4. The EOS parameters are given in Table 2. The bulk modulus and its first derivative with respect to pressure are similar among the four calculations. The enthalpies of formation of  $\text{Sr}_6\text{Co}_5\text{O}_{15}$  from the oxides, defined by eq 9, for both the FM and NM states are also given in Table 2, with differences of 1.2 and 2.3 kJ/mol-atom with and without GGA+U, respectively. Since the values are negative,  $\text{Sr}_6\text{Co}_5\text{O}_{15}$  is a stable compound relative to these oxides at 0 K. Although there is no experimental data to compare, the result is consistent with the observation that  $\text{Sr}_6\text{Co}_5\text{O}_{15}$  is stable at low temperatures in equilibrium

**Table 3.** Heat Capacity and Entropy of FM and NM  $\text{Sr}_6\text{Co}_5\text{O}_{15}$  with the GGA+U Correction As Predicted by the Debye–Grüneisen Model, Per Mole of Atoms

<i>T</i> [K]	FM+U		NM+U	
	<i>C<sub>p</sub></i> [J/mol/K]	<i>S</i> [J/mol/K]	<i>C<sub>p</sub></i> [J/mol/K]	<i>S</i> [J/mol/K]
100	5.920	2.221	5.856	2.215
200	16.032	9.757	15.918	9.699
300	21.053	17.348	20.754	17.206
400	23.591	23.791	23.112	23.536
500	25.153	29.238	24.493	28.856
600	26.286	33.932	25.439	33.411
700	27.216	38.059	26.168	37.391
800	28.047	41.752	26.783	40.929
900	28.833	45.105	27.335	44.118
1000	29.605	48.188	27.852	47.027
1100	30.383	51.050	28.351	49.708
1200	31.180	53.733	28.842	52.198
1300	32.007	56.266	29.332	54.529

with  $\text{Co}_3\text{O}_4$ .<sup>7</sup> When GGA+U is used, the enthalpy of formation for  $\text{Sr}_6\text{Co}_5\text{O}_{15}$  becomes less negative by more than half. Similar behavior was observed when using GGA+U for the oxidation energy of  $\text{Co}_3\text{O}_4$ <sup>26</sup> and the enthalpy of formation of  $\text{LaCoO}_3$ .<sup>28</sup> In these cases, the less stable values were closer to experiment than the predicted value without GGA+U. Indeed, the U–J value employed in this work had been determined by fitting to the  $\text{Co}_3\text{O}_4$  oxidation energy.<sup>26</sup>

**Finite-Temperature Properties.** Harmonic phonon calculations were performed on  $\text{Sr}_6\text{Co}_5\text{O}_{15}$ , and the predicted Debye temperatures are shown in Table 2, where the difference between FM and NM is 3 K, without the GGA+U correction. This difference is smaller than that found in  $\text{Co}_3\text{O}_4$ , possibly since  $\text{Co}_3\text{O}_4$  is more strongly magnetic than  $\text{Sr}_6\text{Co}_5\text{O}_{15}$ , as evidenced in the predicted magnetic moments of the Co ions. Likewise, the difference in the scaling parameters for FM and NM  $\text{Sr}_6\text{Co}_5\text{O}_{15}$ , also given in Table 2, are smaller than that in  $\text{Co}_3\text{O}_4$ .

Phonon calculations employing GGA+U for FM  $\text{Sr}_6\text{Co}_5\text{O}_{15}$  resulted in imaginary phonon modes. As a result, no Debye temperature predictions were possible for the FM+U case. However, the results of using GGA+U for AFM  $\text{Co}_3\text{O}_4$  suggest that the effect of U on the predicted Debye temperature is minimal. This is the case for NM  $\text{Sr}_6\text{Co}_5\text{O}_{15}$ , where the difference in the Debye temperature with and without GGA+U is only 10 K. Therefore, the FM Debye temperature with GGA+U will be assumed to be the same as that for FM without GGA+U. This Debye temperature with the EOS parameters from the FM GGA+U calculation will be used to evaluate the scaling parameter in the Debye–Grüneisen model. The predicted entropies and heat capacities for FM and NM with GGA+U are tabulated in Table 3 up to 1300 K, since  $\text{Sr}_6\text{Co}_5\text{O}_{15}$  decomposes by around 1200 K.<sup>5,6</sup> The parameters of the Gibbs energy function for  $\text{Sr}_6\text{Co}_5\text{O}_{15}$  from eq 10 were fitted to these results and the 0 K enthalpy of formation. They are given in Table 4.

The error in the Gibbs energy function of  $\text{Sr}_6\text{Co}_5\text{O}_{15}$  can be estimated by examining the assumptions made in the first-principles calculations. The first is that the magnetic ground state is FM instead of AFM. The energy difference between an AFM ground state and the FM state is not expected to be much larger than the difference

**Table 4.** Parameters of the Gibbs Energy Function for  $\text{Sr}_6\text{Co}_5\text{O}_{15}$  (eq 10), Fitted to the Thermochemical Properties Predicted by the Debye–Grüneisen Model in Tables 2 and 3,<sup>a</sup>

parameter	FM+U	NM+U
A	-5599628	-5546006
B	3693.645	3823.055
C	-602.231	-623.244
D	-0.08953	-0.05591
E	4863524	5287058

<sup>a</sup> Unit for the Gibbs energy function is J/mol-form.

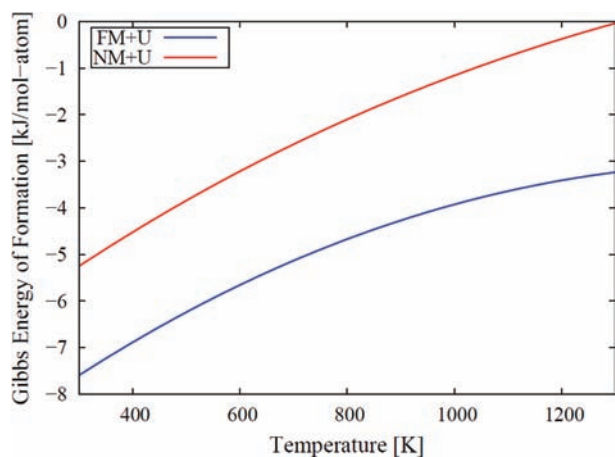


**Figure 5.** Gibbs energy of formation of  $\text{Sr}_6\text{Co}_5\text{O}_{15}$  for the FM+U and NM+U states with respect to  $\text{Co}_3\text{O}_4$ , SrO, and  $\text{SrO}_2$  from CALPHAD modeling.

between FM and NM. By comparing the Gibbs energy functions of the FM and NM states, an estimate for the size of the error can be made. This comparison is shown in Figure 5 and the difference is around 2–3 kJ/mol-atom, approximately constant with respect to temperature. This difference is mostly due to the difference in the enthalpies of formation for FM and NM  $\text{Sr}_6\text{Co}_5\text{O}_{15}$ . However, since the use of GGA+U stabilizes AFM states to very near the ground state, the contribution to this error because of an incorrect magnetic ground state is expected to be much less than the energy difference between the FM and NM states. The mechanical instability of FM with GGA+U, and the subsequent use of the NM with GGA+U Debye temperature, may also contribute error. Error in the thermodynamic stability of a structure with mechanical instability has been reported for pure metals.<sup>43,44</sup> In pure Ti, this error in the 0 K stability was estimated to be 8 kJ/mol-atom.<sup>43</sup> Since NM  $\text{Sr}_6\text{Co}_5\text{O}_{15}$  with GGA+U is predicted to be mechanically stable, the Gibbs energy difference between NM and FM states with GGA+U, 2–3 kJ/mol-atom, discussed earlier as an estimate of the error in predicting the incorrect magnetic structure, also includes an estimate of the error due to the mechanical stability. Another source of error is the magnetic Néel transformation at 25 K. The entropic contribution from this transition is not known experimentally, but can be estimated from the

similar transition in  $\text{Co}_3\text{O}_4$  at 30 K, which contributes 1 J/mol-atom/K to the entropy.

## Summary

A method for determining the Gibbs energy functions for transition metal oxides entirely from first-principles calculations is proposed. The method employs the Debye–Grüneisen model to predict the finite-temperature thermochemical properties, based on the EOS from the energy versus volume curve and the Debye temperature predicted by harmonic phonon calculations. Using  $\text{Co}_3\text{O}_4$  as a test case it is determined that disagreement with experimental data for the heat capacity and entropy is on the order of 1–2 J/K/mol-atom, partly because of ignoring the low-temperature Néel transformation. It is also found that the magnetic state of  $\text{Co}_3\text{O}_4$  and whether the GGA+U approach is used have small effect on the predicted thermochemical properties. The property with the largest effect on the predicted finite-temperature thermochemical properties is the scaling parameter of the Debye–Grüneisen model, which is predicted by harmonic phonon calculations in the current approach. The Gibbs energy function for  $\text{Sr}_6\text{Co}_5\text{O}_{15}$  is then determined. An FM magnetic structure is predicted to be the 0 K ground state, although an AFM state is nearly more stable when GGA+U is employed.

**Acknowledgment.** First-principles calculations were carried out on the LION clusters at the Pennsylvania State University supported by the Materials Simulation Center and the Research Computing and Cyberinfrastructure unit at the Pennsylvania State University. The authors thank Venkateswara Rao Manga and Arkapol Saengdeejeing of the Phases Research Lab at Penn State for fruitful discussions. This paper was written with support of the U.S. Department of Energy under Contract No. DE-FC26-98FT40343. The government reserves for itself and others acting on its behalf a royalty-free, nonexclusive, irrevocable, worldwide license for Governmental purposes to publish, distribute, translate, duplicate, exhibit and perform this copyrighted paper. The United States Department of Energy does not:

- (1) Make any warranty or representation, express or implied, with respect to the accuracy, completeness, or usefulness of the information contained in this report, or that the use of any information, apparatus, method, or process disclosed in this report may not infringe privately owned rights; or
- (2) Assume any liabilities with respect to the use of, or for damages resulting from the use of, any information, apparatus, method, or process disclosed in this report. Reference herein to any specific commercial products, process, or service by trade name, trademark, manufacturer, or otherwise, does not necessarily constitute or imply its endorsement, recommendation, or favoring by the United States Department of Energy. The views and opinions of authors expressed herein do not necessarily state or reflect those of the United States Department of Energy.

(43) Mei, Z. G.; Shang, S. L.; Wang, Y.; Liu, Z. K. *Phys. Rev. B* **2009**, *80*, 104116.

(44) Wang, Y.; Curtarolo, S.; Jiang, C.; Arroyave, R.; Wang, T.; Ceder, G.; Chen, L. Q.; Liu, Z. K. *CALPHAD: Comput. Coupling Phase Diagrams Thermochem.* **2004**, *28*, 79.